EPJ Web of Conferences **129**, 00005 (2016) DOI: 10.1051/epjconf/201612900005
QCD@Work 2016

Gluon fusion contribution to HBB ($B = H, \gamma, Z$) at the LHC

Ambresh Shivaji[1,⋆], *Pankaj* Agrawal[2], and *Debashis* Saha[2]

[1] *INFN, sezione di Pavia, Via Agostino Bassi, 6-27100 Pavia (PV) Italy*
[2] *Institute of Physics, P.O.: Sainik School, Bhubaneswar - 751005, India*

Abstract. We have calculated one-loop amplitudes for the production of Higgs boson in association with two electroweak bosons (H, γ, Z) via gluon-gluon fusion. We present preliminary results for the total cross section at 8, 13 and 100 TeV center-of-mass energies at pp colliders. We study the interference effect and, also comment on the effect of new physics in terms of anomalous couplings of the Higgs boson in these processes.

1 Introduction

There are many standard model (SM) decay or scattering processes which begin at loop-level at the leading order itself. Such loop-induced SM processes are expected to be sensitive to new physics scales. For example, new heavy particles which cannot be produced directly can contribute in the loop in these processes leading to a deviation from the SM predictions. We are particularly interested in loop-induced gluon fusion processes, which can be important at high energy hadron colliders such as the LHC and its future upgrades due to the availability of a large gluon flux.

In the past we have studied $gg \to VVj$, VHj ($V = \gamma, Z, W$) processes at the LHC [1–3]. In this talk we will focus on $gg \to HBB$ ($B = H, \gamma, Z$) processes. Some results on these processes are reported in [4–9]. Observing HHH process would provide us direct information on quartic self-Higgs coupling, while HHZ is a background to HHH in $HHb\bar{b}$ channel. On the other hand, HVV ($V = \gamma, Z, W$) processes are backgrounds to $gg \to HH$ when one of the two Higgs bosons decays into a pair of vector bosons ($\gamma\gamma$, γZ, ZZ^*, WW^*).

The processes under consideration are one-loop at the leading order and proceed via quark loop diagrams. We have triangle, box and pentagon one-loop amplitudes which contribute to them. The one-loop topologies involved are shown in figure 1. In most cases, we can identify prototype amplitudes and generate all other amplitudes by permuting the external momenta and polarizations. Various symmetries can also be utilized to simplify such complex calculations. For example, due to charge conjugation, $\mathcal{M}(gg \to HH\gamma) = 0$. For the same reason in $gg \to HHZ$ case only the axial-vector part of qqZ coupling contributes, while in $gg \to HZ\gamma$ and $gg \to HZZ$ cases only the vector type of amplitude gives non-zero contribution.

2 Calculation and checks

We have calculated the quark loop traces in `FORM` [10] in 4−dimensions. Except top quark, all other quarks are considered massless. The HBB amplitude at this stage is expressed in terms of various

⋆e-mail: ambresh.shivaji@pv.infn.it

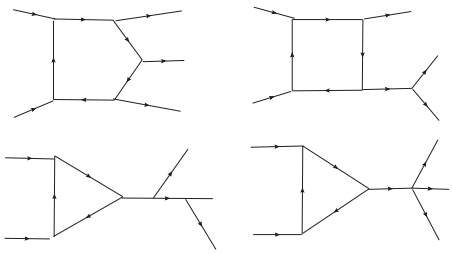

Figure 1. Pentagon, box and triangle topologies contributing to $gg \to HBB$ amplitude. In case of $H\gamma\gamma$ only pentagon contributes, while $HZ\gamma$ does not receive any triangle contribution.

tensor integrals. One of the most difficult parts of one-loop amplitude calculations is the reduction of tensor integrals into a suitable set of scalar integrals. In our processes, we have one-loop five point tensor integral of rank four as the most complicated tensor integral,

$$\mathcal{E}_{\mu\nu\rho\sigma} = \int \frac{d^n l}{(2\pi)^n} \frac{l_\mu l_\nu l_\rho l_\sigma}{D_0 D_1 D_2 D_3 D_4}. \tag{1}$$

Using 4-dimensional *Schouten Identity*, we reduce pentagon tensor and scalar integrals into lower rank box tensor and scalar integrals. For example, the pentagon scalar integral can be written as a linear combination of five box scalar integrals [11, 12]. Reduction of box and lower tensor integrals into appropriate set of scalar integrals is done numerically using the methods of Oldenborgh and Vermaseren (`OV`) [12, 13] in n $(= 4 - 2\epsilon)$-dimensions. Finally, all the required scalar integrals are calculated using the `OneLOop` package [14].

As we expect, the one-loop HBB amplitude is both ultraviolet (UV) and infrared (IR) finite. This is an important check on our calculation. As an ultimate check, we also check the gauge invariance of the amplitude with respect to the gauge currents. This check is done numerically by replacing the polarizations with their respective 4-momenta, $\epsilon_\mu(k) \to k_\mu$ for a given phase space point. We calculate the amplitude numerically before squaring it to get the cross section.

3 Numerical results

We now discuss some preliminary results for our processes at pp colliders. In our calculations we use following SM input parameters,

$$\begin{aligned} M_H &= 125 \text{ GeV}, \; M_Z = 91.188 \text{ GeV}, \; M_W = 80.419 \text{ GeV}, \\ m_t &= 173 \text{ GeV}, \; G_\mu = 1.166389 \times 10^{-5} \text{ GeV}^{-2}. \end{aligned} \tag{2}$$

We also use following basic kinematic cuts to produce results,

$$\mathrm{p_T^{H/Z}} > 1 \text{ GeV}, \; \mathrm{p_T^{\gamma}} > 20 \text{ GeV}, \; |y_{\mathrm{H/Z}}| < 5.0, \; |y_\gamma| < 2.5, \; \Delta\mathrm{R}_{\gamma\gamma} > 0.4. \tag{3}$$

Note that the 1 GeV cut on p_T of H and Z is applied mainly to improve the numerical stability of the code. Further, we have used `cteq6l1` pdf set [15], and have set the partonic center-of-mass energy (cme) as the common scale for renormalization and factorization, $\mu_\mathrm{F} = \mu_\mathrm{R} = \sqrt{\hat{s}}$.

Table 1. SM cross sections at various collider center-of-mass energies with scale uncertainties. All cross sections are in *ab*.

$\sqrt{s}$ (TeV)	8	13	100
$\sigma\,(HHH)$	$7.048^{+34\%}_{-24\%}$	$31.87^{+30\%}_{-22\%}$	$3093^{+17\%}_{-14\%}$
$\sigma\,(HHZ)$	$10.11^{+34\%}_{-24\%}$	$42.76^{+30\%}_{-22\%}$	$3468^{+17\%}_{-14\%}$
$\sigma\,(H\gamma\gamma)$	$1.240^{+37\%}_{-23\%}$	$4.852^{+29\%}_{-22\%}$	$265.8^{+16\%}_{-13\%}$
$\sigma\,(HZ\gamma)$	$1.401^{+32\%}_{-22\%}$	$4.931^{+28\%}_{-21\%}$	$241.3^{+15\%}_{-13\%}$
$\sigma\,(HZZ)$	$83.7000^{+36\%}_{-21\%}$	$471.636^{+36\%}_{-24\%}$	$102573^{+20\%}_{-15\%}$

Table 2. Contributions from pentagon, box and triangle amplitudes at $\sqrt{s}$ = 100 TeV. All cross sections are in *ab*.

	PEN	BX	TR	FULL
$\sigma\,(HHH)$	8110	4319	274.2	3039
$\sigma\,(HHZ)$	17214.5	116996	125552	3468.37
$\sigma\,(H\gamma\gamma)$	265.8	–	–	265.8
$\sigma\,(HZ\gamma)$	78.04	216.2	–	241.3
$\sigma\,(HZZ)$	18677.3	23684.9	31998.7	102573

3.1 SM prediction

In table 1, we report hadronic cross sections for $gg \to HBB$ processes at various collider center-of-mass energies. We also mention the percentage scale uncertainties when the scale is changed by a factor of two around its central value. Due to heavy particles in the final state and presence of many electroweak couplings, these processes have very small cross sections even at 100 TeV. It should be noted that the triangle, box and pentagon amplitudes are separately gauge invariant *with respect to the gluons* in all the processes. To understand the interference effect among these amplitudes, we have computed their individual contributions at the cross section level in table 2. It should be kept in mind that only the full contribution is meaningful and consistent with the complete SM symmetry. We note that except in HZZ case, in all other cases there is a destructive interference between amplitudes. This destructive interference is weakest in $HZ\gamma$ while strongest in HHZ. The HZZ amplitude displays a very strong constructive interference. Similar feature we observe in HWW, however, our calculation is not yet complete [16]. In figure 2 we have selected some kinematic distributions to highlight the variation of the interference effect between amplitudes with respect to a scale like p_T.

3.2 Higgs Anomalous couplings

New physics beyond the SM can induce modifications to couplings among SM particles. The couplings of the Higgs boson with heavy fermions, massive gauge bosons and the Higgs self couplings are of particular interest in this regard. To demonstrate the effect of modifying Higgs couplings in our processes, we have scaled the SM Higgs couplings by factor C_i ($i = ttH,\ ZZH,\ ZZHH,\ 3H,\ 4H$). In table 3 we report the percentage deviation in total cross section when C_i is changed by $\pm 10\%$ from

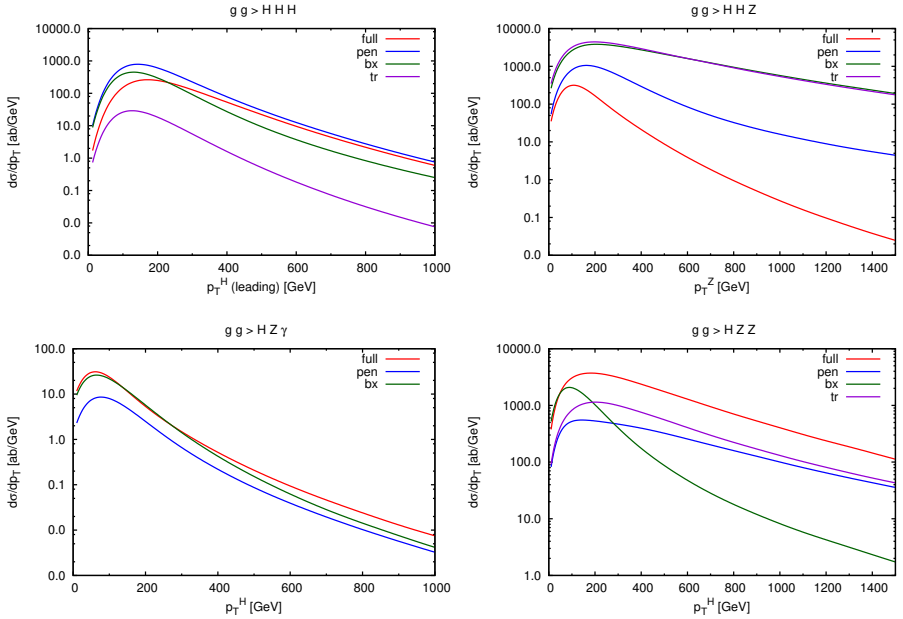

Figure 2. A comparison among various pieces of the amplitude at the level of kinematic distributions in $gg \to HBB$ processes.

its SM value ($C_i^{\rm SM} = 1$), which is consistent with current LHC data on Higgs. We modify one coupling at a time which indeed provides valuable information on its role in changing the interference pattern among various diagrams. The table can be more or less understood with the help of table 2 which has the information on triangle, box and pentagon contributions which in presence of anomalous couplings depend on C_i in a specific manner. We can see that some of our processes are quite sensitive to modifications in ttH and ZZH couplings. Note that we have ignored correlations among the couplings which may arise in a given model of new physics or in presence of higher dimensional operators introduced to capture new physics [16].

4 Conclusion

We have computed loop-induced gluon fusion contributions to HBB ($B = H, \gamma, Z$) processes at pp colliders. One would like to observe HHH to probe the quartic self-coupling of the Higgs boson. Others are also backgrounds to double Higgs production which carries the direct information on the trilinear self-coupling of the Higgs boson. We find that due to small rates, their observation would require a very large luminosity. Some of these processes display a strong interference between different classes of diagrams. We have seen that any modification to the SM Higgs couplings due to new physics effects can spoil the interference and lead to a very different prediction. The effect of anomalous couplings can be studied more systematically using higher dimension operators which would inherently take care of possible correlations among various Higgs couplings.

Table 3. The effect of changing various couplings by 10% of their SM values at $\sqrt{s}$ = 100 TeV. The first and second entries in each parentheses correspond to C_i = 0.9 and 1.1 respectively.

ANML (0.9,1.1)	C_{ttH}	C_{3H}	C_{4H}	C_{ZZH}	C_{ZZHH}
HHH	$(-52\%, +92\%)$	$(+8\%, -5\%)$	$(+1\%, -1\%)$	–	–
HHZ	$(+22\%, +81\%)$	$(-1\%, +1\%)$	–	$(+127\%, +140\%)$	$(-6.3\%, +18\%)$
$H\gamma\gamma$	$(-1\%, +1\%)$	–	–	–	–
$HZ\gamma$	$(-4\%, +4\%)$	–	–	$(-15\%, +15\%)$	–
HZZ	$(-21\%, +25\%)$	$(+0.5\%, -0.4\%)$	–	$(-26\%, +34\%)$	$(+4\%, -3\%)$

References

[1] P. Agrawal *et al.*, Phys. Rev. D **86**, 073013 (2012).
[2] P. Agrawal *et al.*, JHEP **1301**, 071 (2013).
[3] P. Agrawal *et al.*, Phys. Lett. B **741**, 111 (2015).
[4] T. Plehn *et al.*, Phys. Rev. D **72**, 053008 (2005).
[5] T. Binoth *et al.*, Phys. Rev. D **74**, 113008 (2006).
[6] S. Mao *et al.*, Phys. Rev. D **79**, 054016 (2009).
[7] F. Maltoni *et al.*, JHEP **1411**, 079 (2014).
[8] V. Hirschi *et al.*, JHEP **1510**, 146 (2015).
[9] A. Papaefstathiou *et al.*, JHEP **1602**, 006 (2016).
[10] J. A. M. Vermaseren, math-ph/0010025.
[11] W. L. van Neerven *et al.*, Phys. Lett. B **137**, 241 (1984).
[12] A. K. Shivaji, arXiv:1305.4926 [hep-ph].
[13] G. J. van Oldenborgh *et al.*, Z. Phys. C **46**, 425 (1990).
[14] A. van Hameren, Comput. Phys. Commun. **182**, 2427 (2011).
[15] P. M. Nadolsky *et al.* Phys. Rev. D **78**, 013004 (2008).
[16] P. Agrawal *et al.*, *in preparation*.